Nuclear Instruments and Methods in Physics Research A259 (1987) 459–465
North-Holland, Amsterdam

DESIGN AND CONSTRUCTION OF A HIGH PRESSURE XENON TIME PROJECTION CHAMBER

M.Z. IQBAL, H.E. HENRIKSON, L.W. MITCHELL, B.M.G. O'CALLAGHAN, J. THOMAS and H.T-k. WONG

Norman Bridge Laboratory of Physics, California Institute of Technology, Pasadena, California 91125, USA

Received 9 March 1987

The design and construction of a 300 l high pressure xenon gas time projection chamber (TPC) is discussed. This detector has been built to perform a sensitive search for double beta decay of ^{136}Xe.

1. Introduction

Neutrinoless double beta decay provides a sensitive test of the properties of the weak interaction. The observation of this process can be interpreted in terms of a massive Majorana neutrino or right-handed currents in weak decays.

Double beta decay can proceed via two channels: the standard second order weak decay $(A, Z) \rightarrow (A, Z+2) + 2e^- + 2\bar{\nu}_e$ (the "2ν mode") and the lepton number nonconserving $(A, Z) \rightarrow (A, Z+2) + 2e^-$ (the "0ν mode"). There is some evidence for double beta decay from geochemical experiments [1–5]. However, to date direct observation experiments have been unable to provide conclusive evidence for neutrinoless double beta decay, although there is a recent suggestion of 2ν events in ^{82}Se [6]. The double beta decay experiment described in this report is designed to probe 0ν lifetimes greater than 10^{23} yr, corresponding to Majorana neutrino mass of ~ 1 eV or right-handed weak current admixture of $\sim 10^{-5}$ in amplitude [7]. Also, it will be sensitive to the 2ν mode, the measured lifetime of which will provide an important check of the nuclear physics calculations which must be used to interpret the 0ν data.

The number of double beta decay candidates is limited [8]. We have chosen to study ^{136}Xe for the following reasons:

a) The natural abundance of ^{136}Xe is 8.87% and it is possible to have a system with a large number of atoms even without isotopic enrichment.
b) The Q value for ^{136}Xe($\beta\beta$) is larger (2.48 MeV) than for most candidates, and thus the decay rate is enhanced due to a favorable phase space factor.
c) Xenon is a good proportional counter gas and it can act as both the source and detector in a time projection chamber.

The idea of the time projection chamber (TPC) is one of the most important developments in particle detection technology in recent years [9]. In a TPC, a charged particle traversing the detector creates a trajectory of ion–electron pairs. The electrons are drifted by a uniform electric field to a plane of anode wires, where charge multiplication occurs and signals are induced in an underlying orthogonal array of conducting strips. Pulses from the anode wires and readout strips can be used together with the timing information to reconstruct the entire three-dimensional trajectory.

In order to probe 0ν lifetimes $> 10^{23}$ yr, the experiment needs to be sensitive to ~ 1–10 0ν decays per year. A TPC is particularly useful for such a sensitive search, since excellent background rejection can be achieved by track recognition, energy loss (dE/dx) and total energy measurements.

2. Experimental objectives

2.1. Trajectory reconstruction

Track reconstruction provides a powerful method of background suppression. There are several schemes to do this, but in most cases the X–Y information is extracted from a set of independent anode wires and an orthogonal set of readout strips. Since we plan to measure the energy from the proportional charge collection from the anode, we have all the anode wires connected together. In this configuration the X–Y information has to be extracted from a single readout plane. This is achieved by an orthogonal array of copper strips etched on a circuit board as described later. We have performed a detailed Monte Carlo simulation [10] which shows that electron trajectories in high pressure xenon exhibit a large amount of multiple scattering (fig. 1). If the origin of the track is to be identified from the reconstructed trajectory, a spatial resolution of ~ 3–10 mm is required.

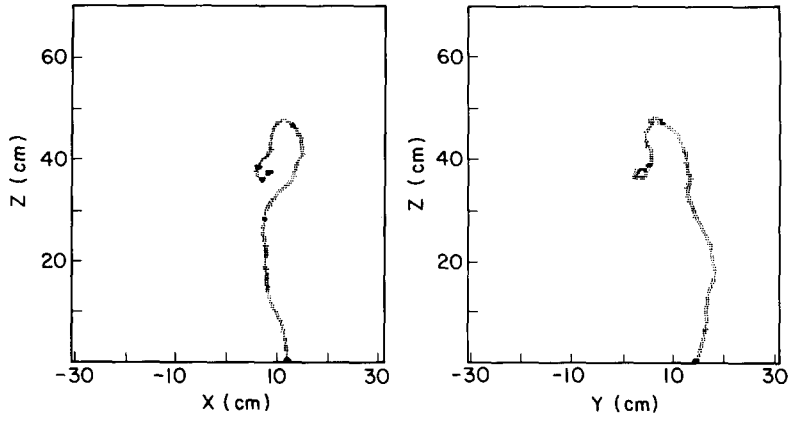

Fig. 1. Monte Carlo simulation [10] of a double beta decay event at 5 atm of xenon assuming the two level discrimination of the present electronics.

2.2. *dE / dx measurement*

The angular correlation of the two electrons in double beta decay, together with the multiple scattering at 5 atm, make reliable identification of the vertex almost impossible. It is thus difficult to distinguish between single-electron and two-electron tracks on the basis of track reconstruction alone, however additional information can be gained from a measurement of dE/dx. An electron scatters more at the end of the trajectory, and has an increased charge deposition which produces a charge "blob". A single electron trajectory has a blob at one end only, whereas a fully contained double beta decay event has a blob at each end. Our 16-channel prototype TPC [11] did not have sufficient resolution to study charge blobs, however our Monte Carlo simulation shows that, with 3 mm resolution in all directions, the charge deposited in the bins in the last centimeter of a trajectory is at least four times larger than the average charge deposited along the trajectory. This suggests that a readout system of two threshold levels, instead of full digitization, should be able to distinguish the charge blobs with good efficiency. We have adopted such a two-level system for the present electronics, however the design is flexible enough to incorporate full digitization, if necessary, with minimum inconvenience.

2.3. *Energy measurement*

Neutrinoless double beta decay of ^{136}Xe produces two electrons with total energy 2.48 MeV. In order to separate this signal from that of the 2ν mode (which has a broad spectrum peaked at 0.8 MeV and a tail extending to 2.48 MeV) and from background events, good energy resolution is desirable. The energy is measured by integrating the signals from the anode wires during the drift time, and we consider a resolution of 5% at 2.5 MeV to be a realistic goal.

3. Design of the time projection chamber

Fig. 2 shows a schematic diagram of the high pressure xenon time projection chamber and its associated gas handling and purification system. Details of the design of the TPC are discussed in this section.

3.1. *Pressure*

The primary requirement of a double beta decay experiment is to build a detector which contains a large number of candidate nuclei and has reasonable efficiency. These requirements suggest a very high pressure for a gas TPC. However, at high pressure the electron trajectories are shorter (due to the higher probability of multiple scattering) and, since spatial resolution is primarily limited by electron diffusion, trajectory information may be lost. Our Monte Carlo simulation suggests a pressure of 5–10 atm to be a practical range for a high pressure xenon TPC. There are other considerations which limit the pressure to less than ~ 10 atm: at higher pressures the attenuation of the drifting electrons by contaminants (which varies as the square of pressure) becomes non-negligible, and the high voltages required for the drift field and for proportional multiplication become difficult to handle.

3.2. *Volume*

The lower limit for the active volume is fixed by the efficiency requirement, since few double beta decay events will be fully contained if the volume is too small. The Monte Carlo simulation of double beta decay events indicated that at 5 atm 20% of events are fully contained in a cylindrical volume with height and diameter of 60 cm. The efficiency increases to more than 50% if the same volume is operated at 10 atm. For the present TPC, a cylindrical active volume of 60 cm in diameter

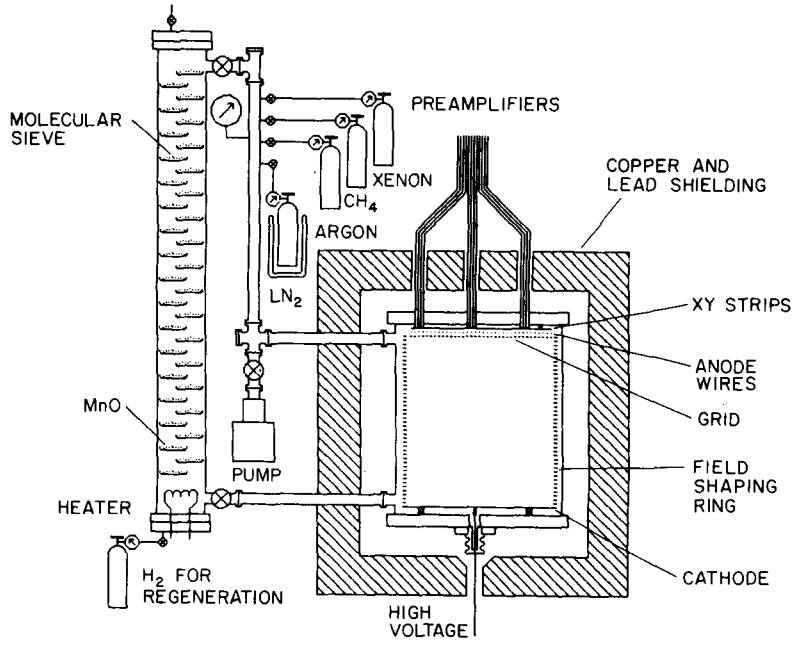

Fig. 2. Schematic diagram of the high pressure xenon TPC.

and 70 cm in height was chosen. There is a gap of 5 cm from the inner wall in all directions to protect against high voltage breakdown.

3.3. Main chamber

The main chamber of the TPC is a cylindrical OFHC copper vessel of 70 cm diameter, 75 cm height and 5 cm wall thickness. The vessel has been designed to withstand a pressure of 15 atm but will operate at 10 atm maximum. The lower cover contains the high voltage feedthrough to the cathode, while the readout system, consisting of the grid, anode wires, guard wires and the XY copper strips, is mounted beneath the top cover.

3.4. Gas composition

Pure xenon is not suitable for a TPC for various reasons [11]. A quenching gas must be added to reduce electron diffusion, increase drift velocity and enhance stability against high voltage breakdown during charge multiplication. 5–10% of CH_4 as the quenching gas was found to be suitable for this experiment. For example, a 5% admixture of CH_4 increases the drift velocity from 1 mm/μs to 1 cm/μs in an electric field of 200 V/cm atm, and also reduces the diffusion by a factor of 10 [12].

3.5. Gas purification

The performance of the detector is degraded by electronegative contaminants (O_2, H_2O, etc.) which attenuate the drifting secondary electrons. To keep the attenuation below 1% at 5 atm, contamination must be below 0.5 ppm, and so continuous purification is necessary. The xenon is purified by passing it over MnO and a molecular sieve (at room temperature) to remove oxygen and water vapor respectively. However, commercial molecular sieve contains a significant amount of ^{238}U and ^{232}Th which creates background by outgassing radioactive ^{222}Rn and ^{220}Rn. The alternative of using a chemically pure binder with the zeolite is being studied. When overloaded, the system can be regenerated by reducing in hydrogen at 300 °C. The gas is circulated by convection from a purification tower of 1.5 m height and 15 cm in diameter. The total volume of the gas can be circulated through the purifier once every 15 min.

3.6. Gas handling

The system has a gas manifold to which is attached a turbomolecular pump, a gas analyzer [13] (to monitor the gas composition), pressure gauges and cylinders of xenon, argon and methane. The system is evacuated to high vacuum before introducing the fill gas, which, in the case of xenon, can be recovered from the system by immersing the xenon cylinder in liquid nitrogen.

3.7. Electric field strength

For most TPCs, a large drift field is important because it increases the drift velocity, and charge can be swept away as soon as possible. In the high pressure xenon TPC, this is not crucial since double beta decay is

a low count rate experiment. In fact, a small drift velocity allows slower electronics and better spatial resolution along the drift direction. However, the diffusion of secondary electrons is a more serious problem at these lower drift velocities. An acceptable 1 cm/μs drift velocity and 2 mm diffusion over a drift distance of 50 cm at an operating pressure of 5 atm will require a voltage of ~ 60 kV at the cathode.

3.8. Electric field uniformity

The electric field inside the active volume of the TPC must be uniform to ensure that all secondary electrons drift parallel to the axis and at constant velocity. This is achieved by layers of field shaping rings at the edge of the detector. A calculation revealed that rings of 0.15 cm thickness separated by 0.5 cm give a field of nonuniformity of less than 0.1% everywhere. This corresponds to trajectory distortion well below the maximum diffusion width of 2 mm.

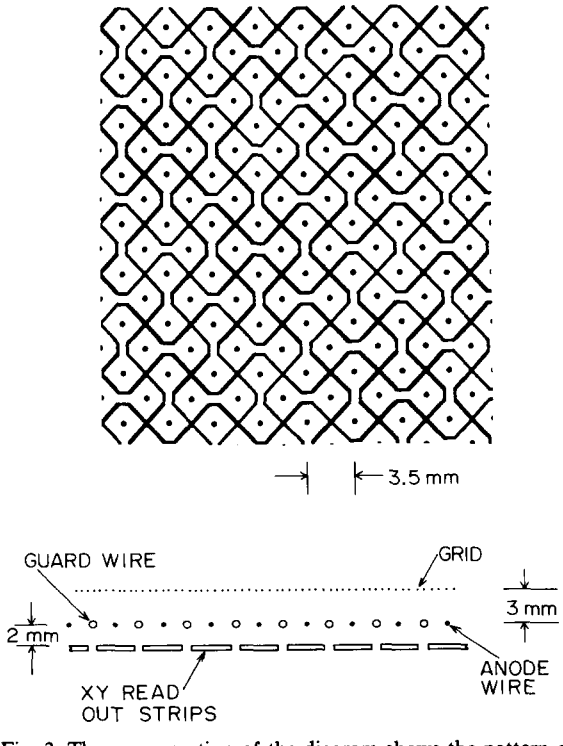

Fig. 3. The upper section of the diagram shows the pattern of the $X-Y$ readout system. The black lines represent regions where the copper has been etched off the circuit board, while the dots represent the plated through holes. The X channels are shown horizontal and the Y channels vertical. The lower section of the diagram shows the relative position of the grid, guard wires, anode wires and $X-Y$ readout strips.

3.9. Anode wires

The anode wires are 0.0025 cm diameter copper wire separated by 3.5 mm as shown in fig. 3. There is a guard wire between each pair of anode wires to enhance proportional multiplication and to ensure that charge multiplication at a point triggers only those strips directly underneath. A 95% transparent grid between the anode wires and the drift region isolates the readout strips from the cathode. The anode wires are connected via a single current sensitive preamplifier to a transient recorder (LeCroy TR8837F), which provides energy information during the drift time. The transient recorder output can be integrated to get the total energy of any event, thereby eliminating the problem of calibrating several hundred preamplifiers individually.

3.10. X–Y readout

The design of the $X-Y$ readout system is shown in fig. 3. This was etched on one side of a copper-clad Rexolite [14] board. An identical pattern, shifted by one unit horizontally, is etched on the other side of the circuit board, and plated-through holes connect the two sides to make the channels continuous. Adjacent channels are separated by 3.5 mm (this defines the best achievable $X-Y$ resolution), and the whole pattern fills a circle of 60 cm diameter, giving 168 channels for each of the X and Y axes. The spacing between the board and the anode wires is 2 mm. For a drift velocity of 1 cm/μs and sampling time of 125 ns, the resolution in the drift direction will be ~ 1.25 mm.

3.11. Proportional multiplication

A multiplication of 10^3–10^4 is adequate, corresponding to an anode potential of less than 5 kV at 5 atm at the present configuration.

3.12. Veto system

There are three hardware vetos for reducing background events. The first is a 2 mm veto ring around the outside of the $X-Y$ readout strips: every time a trajectory crosses the cylindrical boundary the signal will be used to veto the incomplete event. The second veto will be an energy cut: since we expect ^{85}Kr to be the dominant background at energies below the endpoint at 683 keV, all events below this energy will be vetoed. Above ground, a 147 cm × 147 cm × 12 cm liquid scintillator panel is used to veto cosmic ray events.

3.13. Shielding

The system has been designed to allow up to 30 cm of copper and lead shielding to surround the main

chamber. The electronics and gas-handling apparatus will be outside this shielding.

3.14. Calibration

The energy signals from the anode wires will be calibrated by known internal conversion sources (e.g. ^{113}Sn, ^{207}Bi). We plan to use a nitrogen laser to check the uniformity of the electric field and to adjust signals from the readout strips. The laser trajectory also gives precise timing and allows accurate measurement of the drift velocity.

4. Signals and data processing

Fig. 4 shows the schematic diagram of the electronics and data acquisition system for the TPC. The electronics [15] consists of three parts: the preamplifiers, the discriminators, and the CAMAC interface.

4.1. Preamplifiers

The preamplifiers use a low noise commercial preamplifier IC (LeCroy TRA1000). These are current sensitive preamplifiers with a gain of 250 mV/μA, and typical noise of 5–10 mV (1% of the signal). Since electronic components often contain significant levels of background radioactivity, the preamplifiers are mounted in a NIM crate 30 cm from the detector, outside the copper and lead shielding. Twelve preamplifiers are mounted on a 20 cm × 30 cm card, and for a complete system we will require 28 such cards.

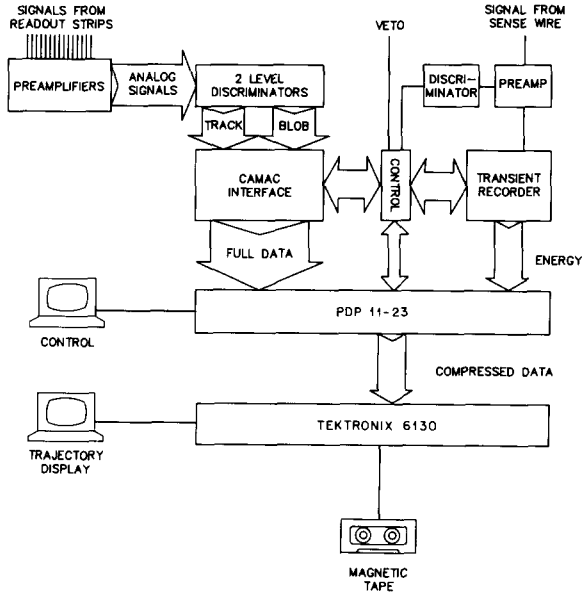

Fig. 4. The schematic diagram of the electronics and the data acquisition system.

4.2. Discriminators

The analog signals from the preamplifiers are fed into two comparators with adjustable threshold levels. One of the comparators produces a TTL signal every time the signal is above noise level, the other produces a signal only when the signal is above a higher threshold corresponding to a charge blob. Forty-eight comparators, handling 24 channels, are designed to fit in a single NIM module, and so 14 such modules are needed for the complete electronics. (The discriminator modules can be replaced by flash ADCs if full digitization is necessary.)

4.3. CAMAC interface

The TTL output of the discriminators is fed into the CAMAC interface boards. These boards are single width CAMAC modules, containing 96K of memory with 48 input lines for 24 channels. One discriminator module requires one CAMAC interface board, and the 14 boards required fit in a single CAMAC crate. Each board is capable of running at 10 MHz rate and stores 200 μs of information. The board can be initiated by CAMAC commands and starts storing information when triggered by the signal from the sense wire. An external veto can be fed to the circuit to reject an event. The memory size is programmable. Multiple events can be stored for diagnosis of delayed events. The 48-line memory is divided into two blocks, one for signals above noise and the other for blobs signals. Each block generates its own LAM signal so that a particular block without any data can be ignored to save reading time.

4.4. Data acquisition system

A PDP 11-23 computer is used as the front end processor to read the CAMAC interface boards, suppress the nonfiring channels (thereby compressing the data by a factor of ~ 100) and then to assemble the data into a four-dimensional array of X, Y, Z (time) and charge. With 2 bits of data per channel, the PDP 11-23 can handle 5–10 events per second. The compressed data is sent to a Tektronix 6130 computer at a rate of about 3K bytes per second. This consumes ~ 3% of the CPU time, the rest of the time is available for on-line data analysis. Events which survive various cuts are stored permanently on magnetic tape. For diagnostic purposes, there is an on-line display of the trajectory and during operations various histograms will be made from all the channels to monitor accidental failure of a channel.

5. Background

For low count rate experiments like the double beta decay search, reducing and understanding backgrounds is critical. To minimize the background from natural radioactivity, the chamber is fabricated from OFHC copper and shielded by additional copper and lead, and all internal components are made of low background materials [16]. However, there are still some sources of background.

5.1. Cosmic rays

The rate of muon-induced events in the TPC without overhead shielding is $\sim 100\ s^{-1}$. The veto ring surrounding the readout pads and the veto scintillators will reject most of these events before they are processed, and so their only contribution is 60 ms per second to the system dead time. A more serious problem is muon capture in the copper and lead shielding. This process can produce neutrons which will, when captured, produce high energy gamma rays. The gamma rays can then interact to produce electrons in the chamber (see below). To reduce this muon-induced background, we plan to install the TPC underground in the St. Gotthard tunnel in Switzerland, where the overburden provides ~ 3000 m water equivalent of shielding and will cut down the muon flux by a factor of $\sim 10^6$.

5.2. ^{85}Kr

Commercially available xenon contains ~ 15 ppm of krypton, about 1 part in 10^{12} of which is ^{85}Kr, a beta emitter with endpoint energy of 0.68 MeV and half-life of 10.7 yr. This will give a low energy background at the rate of about one event per second in our system. We plan simply to reject any event below the ^{85}Kr endpoint energy, but if necessary the krypton contamination can be further reduced by fractional distillation.

5.3. Gamma rays

Despite the low background materials used and the elaborate shielding, there will be gamma-ray-induced background due to natural radioactivity from sources both internal and external to the TPC. The major contribution to the background are electrons produced in the chamber by Compton scattering. However, most single-electron trajectories can be rejected as they will not have charge blobs at both ends, although they do give rise to electronic dead time and cost computer CPU time for data analysis. The gamma-ray-induced background events that we anticipate include:

(a) *Pair production*. Since we cannot distinguish electrons from positrons in our TPC, a pair production event will look similar to a double beta decay event. However, the angular correlation and energy division between the particles is somewhat different for the two processes, and this may allow some cuts to be made to separate the real events from background. Moreover, 10% of the 511 keV gamma rays from the positron annihilation will produce a Compton electron inside the TPC, thereby allowing further rejection of pair production events.

(b) *Compton electrons with initial charge blobs.* Compton electrons may produce energetic secondary electrons (δ-rays) or give abnormally high charge accumulation at the beginning of trajectories. Our Monte Carlo calculation showed $\sim 5\%$ of Compton electrons have charge blobs in the first 5 mm of the track, making it difficult to distinguish these from real events. For these cases, we have to look for an increase in the second derivative of the trajectories at both ends: single-electron events will have a low second derivative at the beginning of the track.

(c) *Double Compton scattering.* The photon following a Compton scattering can scatter again within 3 mm (the resolution of the TPC) so that the two trajectories cannot be separated.

(d) *Compton followed by Auger.* Compton scattering of a photon on the K-shell electrons can be followed by the emission of an Auger electron, which will mimic a double beta decay event.

The probability that an incoming photon will produce an event inside the TPC at 5 atm of xenon has been estimated. Processes (a) and (b) dominate the other background events by three orders of magnitude. In table 1 we show the number of background events which we expect in the TPC from these processes. To estimate the absolute gamma flux entering the TPC, we used the results of the Caltech ^{76}Ge double beta decay experiment [17] at Caltech and in the St. Gotthard tunnel, and scaled for the efficiency and volume of the TPC. Furthermore we assumed an energy resolution of 5% (125 keV at 2.5 MeV), and that a pair production event or a Compton electron with a charge blob at the beginning of the trajectory cannot be distinguished from a real event.

Table 1
Estimated number of background events in TPC in one year running at 5 atm

Background		0.8 MeV (width 0.125 MeV)	2.5 MeV (width 0.125 MeV)
Pair production	above ground	19700	1250
	tunnel	500	10
Compton electrons with initial blob	above ground	10200	50
	tunnel	680	1.3

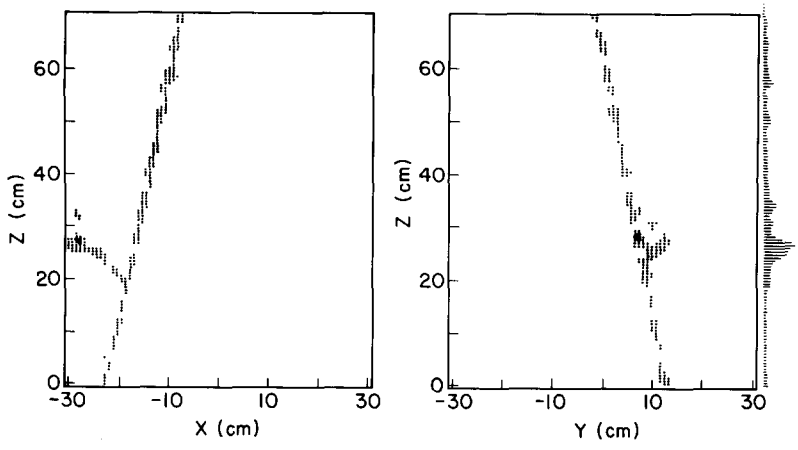

Fig. 5. The XZ and YZ projection of a cosmic ray muon ejecting a delta electron, Z being the drift direction. The energy of the muon is shown as a function of the drift time on the right hand side. The fill gas was Ar with 10% CH_4 at 2 atm, and the drift field 300 V/cm.

6. Estimation of lifetime limits of ^{136}Xe

Using the 2.5 MeV background estimation from table 1, the 0ν mode lifetime and Majorana neutrino mass limit [7] that the TPC can set after running for a year at 5 atm are

above ground: $\tau^{0\nu} \geq 1.3 \times 10^{22}$ yr,
$m_\nu \leq 4.8$ eV;
underground: $\tau^{0\nu} \geq 1.5 \times 10^{23}$ yr,
$m_\nu \leq 1.4$ eV.

7. Conclusion

The high pressure gas TPC is now running as a detector. Half of the electronics has been constructed, and at present adjacent channels of the readout system are connected to give 7 mm spatial resolution. For diagnostic purposes, we are using an argon–methane mixture to test the electronics and study backgrounds. The performance is quite promising as can be seen from a typical cosmic ray muon trajectory shown in fig. 5. Once we have a complete xenon recovery system, we will begin test runs with xenon at various pressures. To save time and have more flexibility during the diagnostic stage, we have used available materials in some places. We have started replacing these temporary parts with components made from low background materials. We have also started making the remainder of the electronics. By the spring of 1987, we plan to have the high pressure xenon time projection chamber collecting data.

Acknowledgements

We would like to thank Felix Boehm for many illuminating discussions, and Michael Douglas, John Gehring and Ryoji Watanabe for their contributions to the data acquisition software.

References

[1] T. Kirsten and H.W. Muller, Earth Planet. Sci. Lett. 6 (1969) 271.
[2] M.G. Inghram and J.H. Reynolds, Phys. Rev. 78 (1950) 822.
[3] T. Kirsten, O. Schaeffer, E. Norton and R. Stoenner, Phys. Rev. Lett. 20 (1968) 1300.
[4] E.W. Hennecke, O. Manuel and D. Shabu, Phys. Rev. C11 (1975) 1378.
[5] E.W. Hennecke, Phys. Rev. C17 (1978) 1168.
[6] S.R. Elliott, A.A. Hahn and M.K. Moe, Phys. Rev. Lett. 56 (1986) 2582.
[7] K. Grotz and H.V. Klapdor, Phys. Lett. B157 (1985) 4.
[8] See, e.g., W.C. Haxton and G.J. Stephenson, Progr. Part. Nucl. Phys. 12 (1984) 409.
[9] D.R. Nygren, 198 PEP (1975).
[10] M.Z. Iqbal, B.M.G. O'Callaghan and H.T-k. Wong, Nucl. Instr. and Meth. A253 (1987) 278.
[11] M.Z. Iqbal, B.M.G. O'Callaghan, H.E. Henrikson and F. Boehm, Nucl. Instr. and Meth. A243 (1986) 459.
[12] A. Peisert and F. Sauli, CERN 84-04.
[13] Dycor Electronics Inc.
[14] Rexolite 1422, Oak Materials Group Inc.
[15] M.Z. Iqbal et al., to be published.
[16] See, e.g., G.F. Knoll, Radiation Detection and Measurement (Wiley, New York, 1979).
[17] A. Forster, H. Kwon, J.K. Markey, F. Boehm and H.E. Henrikson, Phys. Lett. B138 (1984) 301; P. Fisher, in: 6th Moriond Workshop, eds., O. Fackler and J. Tran Thanh Van (Frontières, Paris, 1986).